Fabrication of Self-Assembled Nanoporous Templates for Applications to Patterned Media Recording

Jia-Yang Juang and David B. Bogy

Computer Mechanics Laboratory

Department of Mechanical Engineering

University of California at Berkeley

Berkeley, CA 94720

ABSTRACT

Ordered nanoporous alumina templates were fabricated by self-assembly technology. A two-step anodization process was also carried out to obtain templates with straight pores without removing the aluminum and barrier layer. Polycrystalline structure was observed with a grain size of about two micrometers in which the pores were almost perfect hexagonally ordered. The pore arrays exhibit different orientation along the boundaries of neighboring grains. Nanopatterning implemented by electron-beam lithography demonstrates a potential for writing concentric circular patterns with linewidths as small as 30 nm.

1. INTRODUCTION

The areal density in magnetic storage media, especially for hard disk drives, is expected to reach a physical limitation known as the superparamagnetic limit because of thermal instability. Patterned media has been proposed as one solution to overcome this limitation [1]. Unlike current magnetic recording, which uses continuous granular media, patterned media domains are discrete. The bits on the media are physically isolated from their neighbors so magnetic interactions are smaller. One terabit per square inch is potentially achievable with a bit size around 25 nm.

The fabrication methods of patterned media can be divided into two categories: One uses IC fabrication techniques, including lithography, magnetic material deposition, and lift-off [2]. But the bit arrays with sub micron or even tens of nanometer feature sizes are too small to be defined by conventional optical lithography. Advanced non-optical lithography technology, such as electron-beam, imprinting, X-ray, ion-beam, and interference lithographies, will be required. The main drawback of this approach is that the aspect-ratio of the data bit is limited to be around one.

The other approach used to fabricate patterned media is by self-assembled nanostructures. Semiconductor nanowire arrays, such as silicon and zinc oxide, have been grown by CVD based on the vapor-liquid-solid (VLS) mechanism [3]. Unfortunately, there is no similar way to grow high-aspect ratio magnetic nanowires. Sun et al. [4] demonstrated the synthesis of monodisperse iron-platinum (FePt) nanoparticles with tunable diameter from three to ten nanometers. Another alternative is to use self-assembled nanoporous structure as templates to grow magnetic nanowires within the pores, which has been investigated by

several research groups [5-11]. In this report, we focus on the fabrication of porous alumina templates.

Porous oxide growth with a hexagonal pore arrangement on aluminum under anodic bias in various dilute acids has been studied for more than 40 years [12, 13]. Figure 1 shows schematically the hexagonally ordered pore arrangement. However, the underlying pore arrangement mechanism is still not well understood. One likely explanation is that, due to the expansion of the aluminum during the anodization, the alumina, which is inherently porous, will form with minimum energy. The hexagonal honeycomb structure is one of the close-packed, robust, and minimum forming energy structures found in nature, and it is expected to be obtained after the anodization of aluminum foil with a smooth surface under proper anodization conditions. Straight alumina channels are formed as the aluminum ions diffuse out of, and oxygen ions diffuse into, the barrier layer under the electric field. Dissolution of the alumina takes place more readily at concave sites due to the concentrated electric field. Thamida *et al.* [14] used linear stability theory and a weakly nonlinear evolution equation to predict the transition from porous to nonporous alumina at a pH equal to 1.77. Broughton and Davies [15] produced a stochastic simulation model, which was used to predict an anodic oxide membrane formation. Jessensky *et al.* [16] proposed the idea that the resulting mechanical stress, caused by the volume expansion of the aluminum at the metal and oxide interface, promotes the formation of ordered hexagonal pore arrays. Zhang et al. proposed a cellular growth mechanism in ordered porous alumina due to oxide propagation at a curved metal-oxide interface [17].

Prepatterning on the aluminum surface with particular features before the anodization process has been successfully used to guide the growth of straight pores. Li *et al.* prepared

hexagonally ordered pore array structures with variable interpore distance based on prepatterning by electron-beam lithography and a subsequent anodization in oxalic acid solution [18]. Liu *et al.* also obtained similar results by prepatterning with focused ion beam lithography [19]. Masuda *et al.* even fabricated a pore array with square or triangular openings based on the two-dimensional tiling of the cell configuration of anodic porous alumina. They also showed that the shapes of the cells and openings were determined not by the shape of the depressions which served as the initiation sites for pore growth but by the arrangement of the initiation sites in two-dimensional space on the aluminum surface [20].

Regularity of the pore arrangement in porous alumina can be increased by increasing the anodizing time under proper conditions [21]. However, the template obtained by prolonged anodization is not suitable for patterned media applications because of the excessive thickness and irregular pore configuration on the top surface. Masuda and Satoh presented a two-step anodizing process to fabricate ordered through-channel arrays with tunable thickness [22].

To our knowledge, a concentric circular pore arrangement in alumina has not been shown, but this could be very useful for the patterned media application. In our study, electron-beam lithography was used as means to produce the concentric circular features.

2. EXPERIMENTAL SETUP AND PROCEDURE

2.1 Self-Assembled Nanoporous Templates

Several similar recipes, with minor differences, for preparing anodic alumina porous templates can be found in the literature [5-13, 18, 20]. The approach used by Keller, O'Sullivan, and Masuda was adopted in this research.

Figure 2 illustrates the scheme of the process for the preparation of self-assembled nanoporous templates. High purity (99.999%) aluminum foils purchased from Goodfellow were used as substrates. After it was carefully ultrasonically cleaned and degreased by acetone, the foil was then electropolished to lower the roughness of the aluminum surface. The electropolishing was conducted under a constant voltage of 3.5 V at room temperature for 10 minutes in a mixture of 60 wt % perchloric acid and ethanol ($HClO_4$: C_2H_5OH= 1: 4 by volume) with aluminum as the anode and copper plate as the cathode. Anodization was performed in 0.3 M aqueous oxalic acid at 40 V and 25 °C for two hours. Anodization is usually carried out at a high voltage in dilute acids at lower temperature in order to promote the growth of larger cells and pores. After anodization, the alumina foil was dipped into a saturated $HgCl_2$ solution to remove the aluminum and keep the porous alumina unharmed. Subsequent etching treatment was conducted in a 5% wt H_3PO_4 solution at 25 °C to remove the barrier layer and, hence, reveal the pores. This helps us to observe the pore arrangement at the bottom of the templates. The experimental setup is shown in Fig. 3.

Figure 4 illustrates a two-step anodization process in which the hexagonally ordered pore configuration can be achieved without removal of the barrier. The detailed process sequence is described as follows. The aluminum foil was degreased with acetone. The first anodization was conducted at a constant voltage of 40 V in a 0.4M aqueous oxalic acid at 25 °C for 18 hours. This alumina was then stripped away by a mixture of H_3PO_4 (6 wt %) and H_2CrO_4 (1.8 wt %) at 60 °C. The remaining periodic concave patterns on the aluminum foil acted as self-assembled masks for the second anodization in which all conditions were the same as those in the first one.

2.2 Nanopatterning

In this study nanopatterning was implemented by use of the Nanometer Pattern Generation System based on electron-beam lithography.

Electron-beam lithography or EBL is a high-resolution patterning technology in which high-energy electrons are focused into a narrow beam and are used to expose electron-sensitive resists point-by-point. Unlike optical lithography, the resolution of EBL is limited by proximity effects. This refers to the tendency of scattered electrons to expose nearby areas that may not be intended for exposure. The scattering can be divided into forward and backscatter. Forward scatter occurs over a small range of angles with respect to the incident velocity and leads to a slight broadening of the image. Backscatter contributes a large area fog of exposure. Commercially available EBL systems are now capable of routinely writing features with resolutions of tens of nanometers. More details on EBL can be found in [23, 24].

"Nanometer Pattern Generation System" or NPGS is an integrated software program, developed by J. C. Nabity [25], for the delineation of complex structures using a commercial electron beam microscope. Patterns are created using DesignCAD, which is a commercial computer-aided-design program.

3. RESULTS AND DISCUSSIONS

Scanning electron microscopy (SEM) and atomic force microscopy (AFM) were used to measure the topography of samples in this study. Figures 6 and 7 show the SEM images of the raw aluminum foil. The stripes on the surface are a result of the manufacturing process. AFM study shows that the root-mean-square (rms) roughness is 37.84 nm over 3 by 3 um area as shown in Fig. 8. The roughness is expected to be even larger over a broader area.

After the electropolishing treatment, the rms roughness was lower to 0.731 nm over one micrometer square area. Figure 9 shows the SEM image of electropolished aluminum foil. The surface topographies of the alumina templates with and without electropolish are shown in Figs. 10 and 11, respectively. Comparing Fig. 10 with Fig. 7, we find that the pores tend to form along the stripes, which reinforces the suggestion made in the previous section. The pore arrangement was more random on the electropolished foils, which indicates the pores grew randomly in the very beginning of anodizaton process.

Figure 12 shows the SEM dissected view of the template before the removal of the barrier layer and Fig. 10, 13, 14, and 15 show the enlargement of each image. The fabrication was conducted with a two-hour anodization according to the process described in Section 2.1. The top and bottom views illustrate the pore configurations in the earlier and later anodization stages, respectively. A polycrystalline convex feature arrangement with domains of about two micrometers is observed on the bottom view as shown in Fig. 13. Within each domain, almost perfect hexagonally arranged convex features are observed. In the domains, each hemisphere is surrounded by six others hexagonally, which are interconnected to form a network structure. The cell size or the center-to-center distance between neighboring hemispheres is about 100 nm, which is consistent with the results obtained by other researchers. This cell size is tunable and is believed to be proportional to the anodizing voltage. More details can be found in the literature [12, 13, and 26].

A transition of pore growth from a crooked to straight pattern can be observed from the cross sections of the templates in Figs. 14 and 15. An additional barrier layer removal and pore-widening etching process was carried out in 5 wt % phosphoric acid at 25 °C for 1.5 hours. The porous template obtained is shown in Fig. 16. The pore arrangement is similar to

that before removal of the barrier layer. The reason the pores are not as ordered as the hemispheres is probably due to the over-etching in the pore-widening process.

Figure 17 shows the “top-view” SEM image of the alumina grown by a two-step anodization. Although the pores are not as clear as those in Fig. 16, which was done by a one-step anodization and removal of the barrier layer, the pore arrangement as well as cell size resembles that in Fig. 16.

In order to look into the feasibility of “guided self-assembly” of porous templates with concentric circular pore arrangements, NPGS accompanied with a scanning electron microscope (JEOL 6400) has been used to write various prepatterns with sub-micrometer scale features. The procedure of pattern writing on polymers is described as follows. A positive poly(methyl methacrylate) (PMMA) electron-sensitive resist with a molecular weight of 950,000 3% in chlorobenzene was spun at 500 rpm for 3 sec then 4000 rpm for 20 sec onto a Si wafer to achieve a thickness of about 150 nm. Then it was baked two hours at 160 °C. After that the test pattern was written on the PMMA at 40 kV, with doses of 2.91 nC/ cm, exposure of 412.1 usec, beam current of 5 pA, and center-to-center distance of exposure points: 7.08 nm. The exposed wafer was developed in 3:1 IPA (Isopropyl Alcohol = 2 Propanol): MIBK (Methl Isobutyl Ketone = 2-Pentanone, 4-methyl) at 25 °C for 70 seconds. The wafer was then immediately rinsed in IPA for about 20 seconds, followed by DI water for about 20 seconds, and then it was blown dry with a clean gas. Figure 18 shows the result of patterning with complex features on PMMA. Figure 19 is an enlargement of Fig. 18, focusing on the concentric circles. The line width of the circles is about 30 nm, which demonstrates the potential of nanopatterning in the applications of patterned media recording.

4. CONCLUSIONS AND FUTURE WORK

Self-assembled nanoporous alumina templates have been fabricated. The interpore distance or cell size is 100 nm, which results in an areal pore density of 64.5 Gigabit per square inch. However, the potential of decreasing the interpore distance to 25 nm provides a promise of ultrahigh areal density up to one Terabit per square. The main strengths of this approach include:

- ✓ Relatively easy to be utilized and cost-effective.
- ✓ The potential to achieve ultrahigh areal density with ordered structure.
- ✓ The interpore distance and pore diameter can be arbitrarily tuned simply by controlling the anodizing voltage and the etching time, respectively.

The main drawbacks are:

- ✓ The self-assembled pore configuration is inherently hexagonally ordered and cannot be designed arbitrarily. Advanced lithography techniques may be required to prepattern the aluminum in order to guide the self-assembly of pore formation.
- ✓ The self-assembly process is not a standard silicon one and more effort may be required to integrate it into IC compatible or hard disk drive facilities.
- ✓ In the applications of patterned media recording, deposition of high quality magnetic materials into the pores needs more emphases. Electroplated magnetic materials may not be a good candidate of high quality recording media.

A two-step anodization process was used to obtain straight through-channels. Self-assembled hexagonally ordered pores were formed after a certain time of anodization. The

irregular alumina was then stripped away, leaving the aluminum with ordered pits on the top surface. A second anodization was then carried out with the help of the ordered pits as a mask. Almost perfect ordered pore arrays were observed within domains of two micrometers.

The result of EBL demonstrates the ability to write complex patterns, including concentric circular ones with linewidths as small as 30 nm. In the future, we will investigate the feasibility of guided-self-assembly to form templates with concentric circular pore arrangements and the applications for information storage.

ACKNOWLEDGEMENT

This study is supported by the Computer Mechanics Laboratory (CML) at the University of California at Berkeley. The first author thanks Stanley Kon for helpful discussions on the anodization experimental setup, Xiaoguang Ma for AFM images of the raw aluminum foils, and Microlab at UC Berkeley for providing facilities.

REFERENCES

1. Hughes, Gordon F., "Patterned media" in "The physics of ultra-high-density magnetic recording," Plumer, M., van Ek, J., and Weller, D. (editors), Springer, 2001.
2. Ross, CA, Smith, HI, Savas, TA, Schattenburg, M., Farhoud, M., et al., "Fabrication of patterned media for high density magnetic storage," *Journal of Vac. Sci. Technol. B*, v. 17, 3168-3176, 1999.
3. Huang, M. H., Mao, S., Feick, H., Yan, H., Wu, Y., Kind, H., Weber, E., Russo, R., and Yang, P., "Room-temperature ultraviolet nanowire nanolasers," *Science*, v. 292, 1877, 2001.
4. Sun, S., Murray, C. B., Weller, D., Folks, L., and Moser, A., "Monodisperse FePt nanoparticles and ferromagnetic FePt nanocrystal superlattices," *Science*, v. 287, 1989-1992, 2000.
5. Tsuya, N., Tokushima, T., Shiraki, M., Wakui, Y., Umehara, Y., Saito, Y., Nakamura, H., Katsumata, Y., Iwasaki, S., and Nakamura, Y., "Magnetic discs using anodic oxidized aluminum substrates," *IEEE Trans. Magn.*, v. MAG-23, 2242- 2244, 1987.
6. Masuda, H., Yotsuya, M., Asano, M., Nishio, K., Nakao, M., Yokoo, A., and Tamamura, T., "Self-repair of ordered pattern of nanometer dimensions based on self-compensation properties of anodic porous alumina," *Applied Physics Letters*, v. 78, 826- 828, 2001.
7. Nielsch, K., Muller, F., Li, A. P., and Gosele, U., "Uniform nickel deposition into ordered alumina pores by pulsed electrodepostion," *Advanced Materials*, v. 12, 582- 586, 2000.
8. Nielsch, K., Muller, F., Liu, G., Wehrspohn, R.B., Gosele, U., Fischer, S. F., and Kronmuller, H., "Magnetic nanowire arrays obtained by electro-deposition in ordered

alumina templates,*" Electrochemical Processing in ULSI Fabrication III , P.C. Andricacos, P.C. Searson, C. Reidsema-Simpson, P. Allongue, J.L. Stickney, G.M. Oleszek, eds. PV-2000-8, Electrochemical* Society, Pennington, 2000.

9. Metzger, R. M., Konovalov, V. V., Sun, M., Xu, T., Zangari, G., Xu, B., Benakli, M., and Doyle, W. D., "Magnetic nanowires in hexagonally ordered pores of alumina," *IEEE Trans. Magn.,* v. 36, 30- 35, 2000.
10. Zheng, M., Menon, L., Zeng, H., Liu, Y., Bandyopadhyay, S., Kirby, R. D., and Sellmyer, D. J., "Magnetic properties of Ni nanowires in self-assembled arrays," *Physical Review B.,* v. 62, 12282- 12286, 2000.
11. AlMawlawi, D., Coombs, N., and Moskovits, M., "Magnetic properties of Fe deposited into anodic aluminum oxide pores as a function of particle size," *Journal of Applied Physics,* v. 70, 4421- 4425, 1991.
12. Keller, F., Hunter, M. S., and Robinson, D. L., "Structural features of oxide coatings on aluminum," *Journal of the Electrochemical Society,* v. 100, 411- 419, 1953.
13. O'Sullivan and Wood, G, C., "The morphology and mechanism of formation of porous anodic films on aluminum", *Proceedings of the Royal Society of London*, v. 317, 511-543, 1970.
14. Thamida, S. K. and Chang, H. C., "Nanoscale pore formation dynamics during aluminum anodization", *Chaos*, v. 12, 240-251, 2002.
15. Broughton, J. and Davies, G. A., "Porous cellular ceramic membranes: a stochastic model to describe the structure of an anodic oxide membrane," *Journal f Membrane Science*, v. 106, 89-101, 1995.

16. Jessensky, O., Muller, F., and Gosele, U., "Self-organized formation of hexagonal pore arrays in anodic alumina," *Applied Physics Letters*, v. 72, 1173-1175, 2001.
17. Zhang, L., Cho, H. S., Li, F., Metzger, R. M., and Doyle, W. D., "Cellular growth of highly ordered porous anodic films on aluminum," *Journal of Materials Science Letters*, v. 17, 291-294, 1998.
18. Li, A. P., Muller, F., and Gosele, U., "Polycrystalline and monocrystalline pore arrays with large interpore distance in anodic alumina," *Electrochemical and Solid-State Letters*, v. 3, 131-134, 2000.
19. Liu, C. Y., Datta, A., and Wang, Y. L., "Ordered anodic alumina nanochannels on focused-ion-beam-prepatterned aluminum surfaces," *Applied Physics Letters*, v. 78, 120-122, 2001.
20. Masuda, H., Asoh, H., Watanabe, M., Nishio, K., Nakao, M., and Tamamura, T., "Square and triangular nanohole array architectures in anodic alumina," *Advanced Materials*, v. 13, 189-192, 2001.
21. Masuda, H., and Satoh, M., "Fabrication of gold nanodot array using anodic porous alumina as an evaporation mask," *Jpn. J. Appl. Phys.*, v. 35, L126-L129, part 2, 1996.
22. Masuda, H., and Fukuda, K., "Ordered metal nanohole arrays made by a two-step replication of honeycomb structures of anodic alumina," *Science*, v. 268, 1466-1468, 1995.
23. Campbell, S. A., The science and engineering of microelectronic fabrication, Oxford University Press, 1996.

24. Rai-Choudhury, P. (editor), Handbook of microlithography, micromaching, and microfabrication, v. 1, microlithography, Bellingham, Wash., USA : SPIE Optical Engineering Press ; London, UK : Institution of Electrical Engineers, c1997.
25. http://www.jcnabity.com/
26. Wehrspohn, R. B., Li, A. P., Nielsch, K., Muller, F., Erfurth, W., and Gosele, U., “Highly ordered alumina films: pore growth and applications,” in Oxide Films, K.R. Hebert, R.S. Lillard, B.R. Mac Dougall eds., PV-2000-4, Electrochemical Society, Pennington, pg.271, 2000.

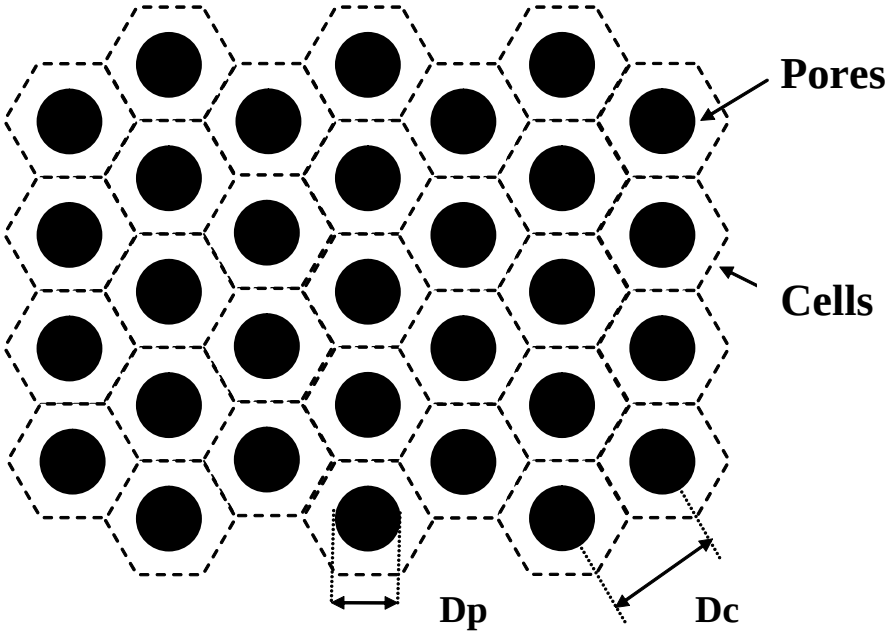

Fig. 1 Ideal hexagonal cell arrangement of a porous alumina template

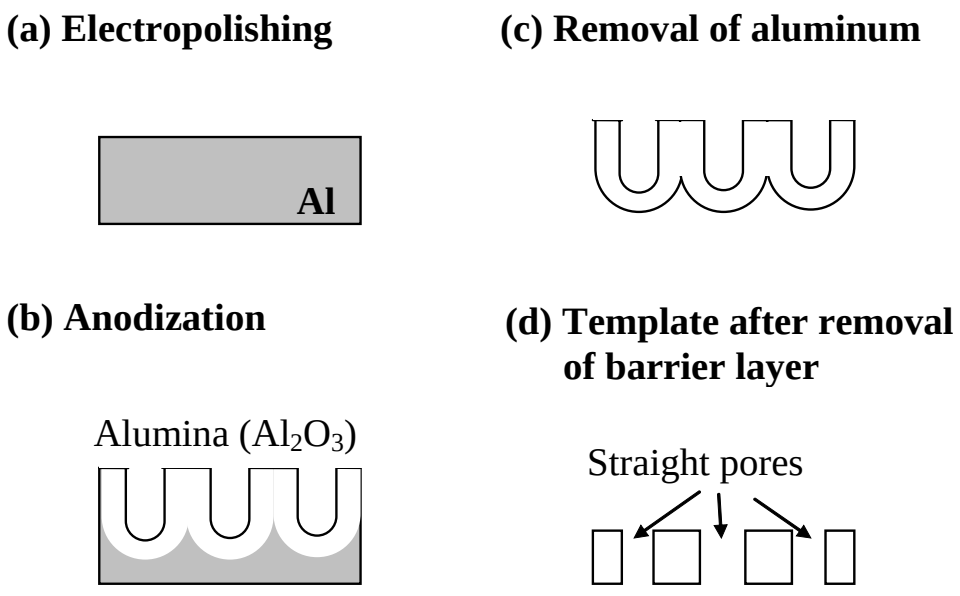

Fig. 2 Schematic process flow of nanoporous templates

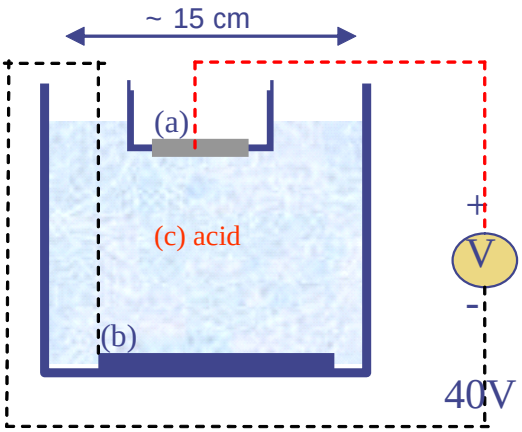

Fig. 3 Experimental setup for anodization of aluminum foils. (a) anode: 0.1 mm Al foil, (b) cathode: copper plate, (c) electrolyte: oxalic acid, 0.3 M (~2.8 wt %), ~25 °C

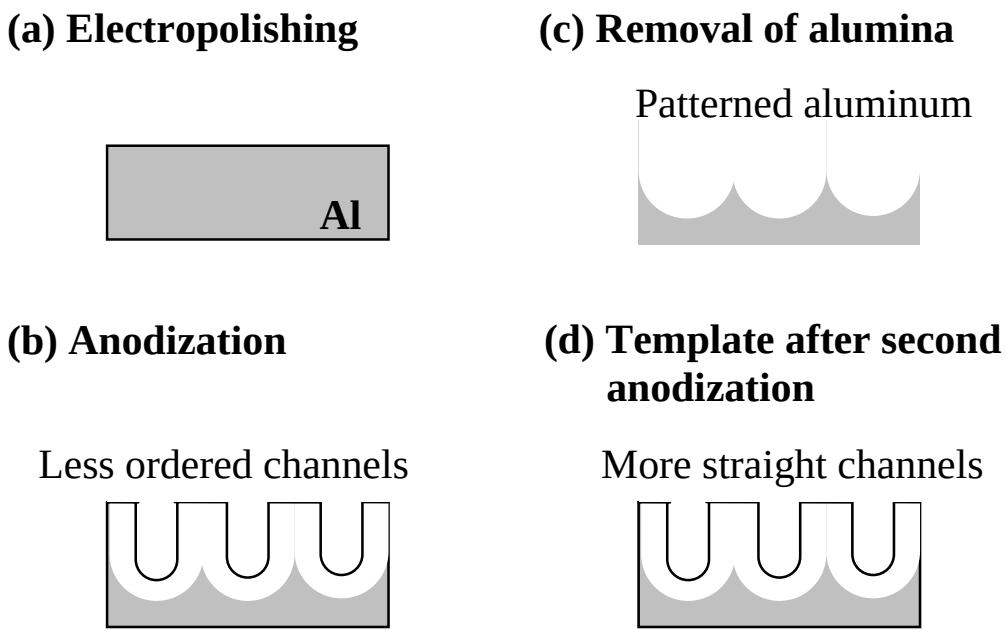

Fig. 4 Schematic process flow of a two-step anodization process for nanoporous templates

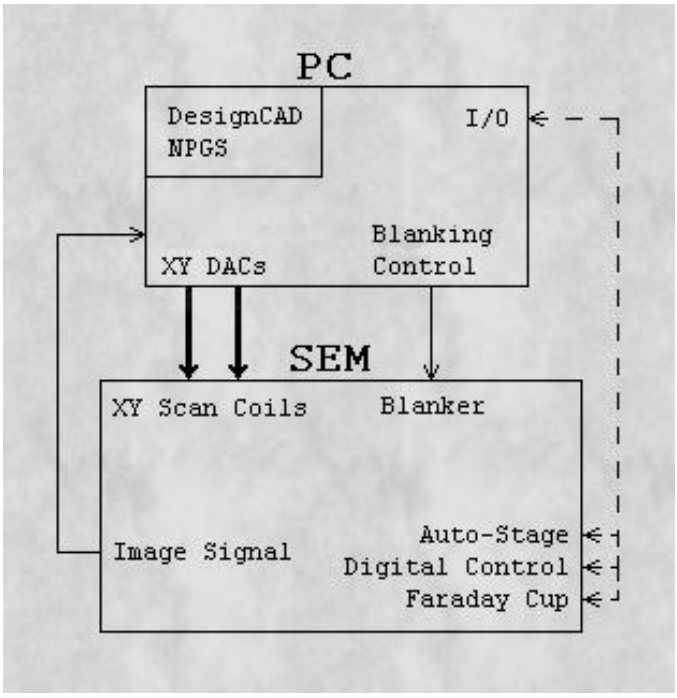

Fig. 5 Schematic diagram of Nanometer Pattern Generation System (NPGS)

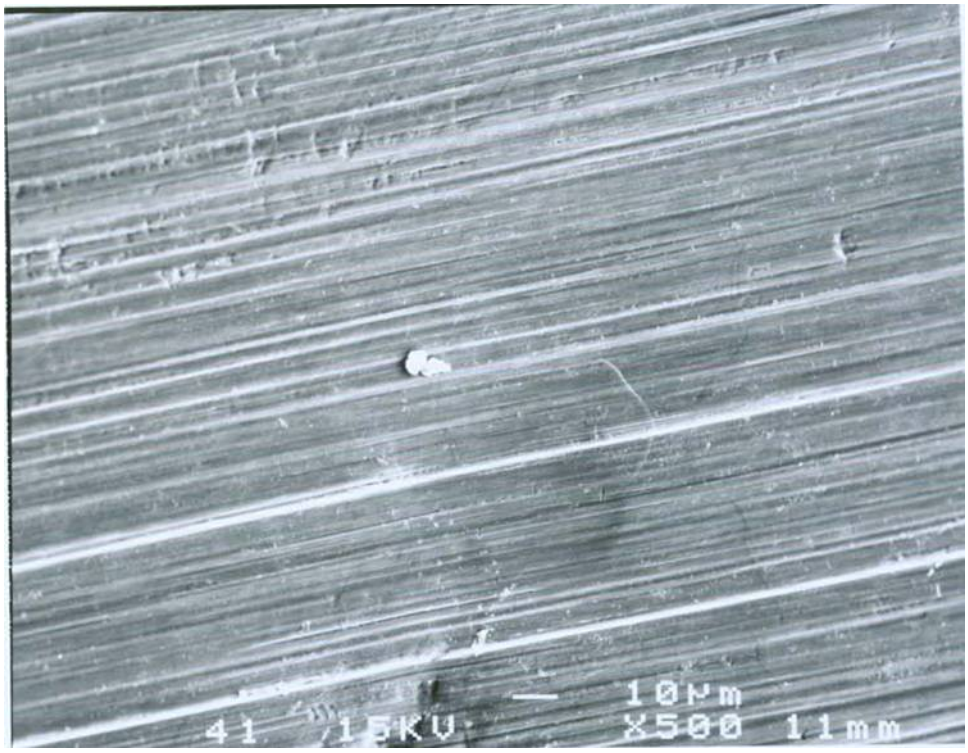

Fig. 6 SEM image of a raw aluminum foil, 500X, Goodfellow Al foil, polycrystalline, 99.999%, 0.1 mm thick, 25x25 mm, temper: as rolled

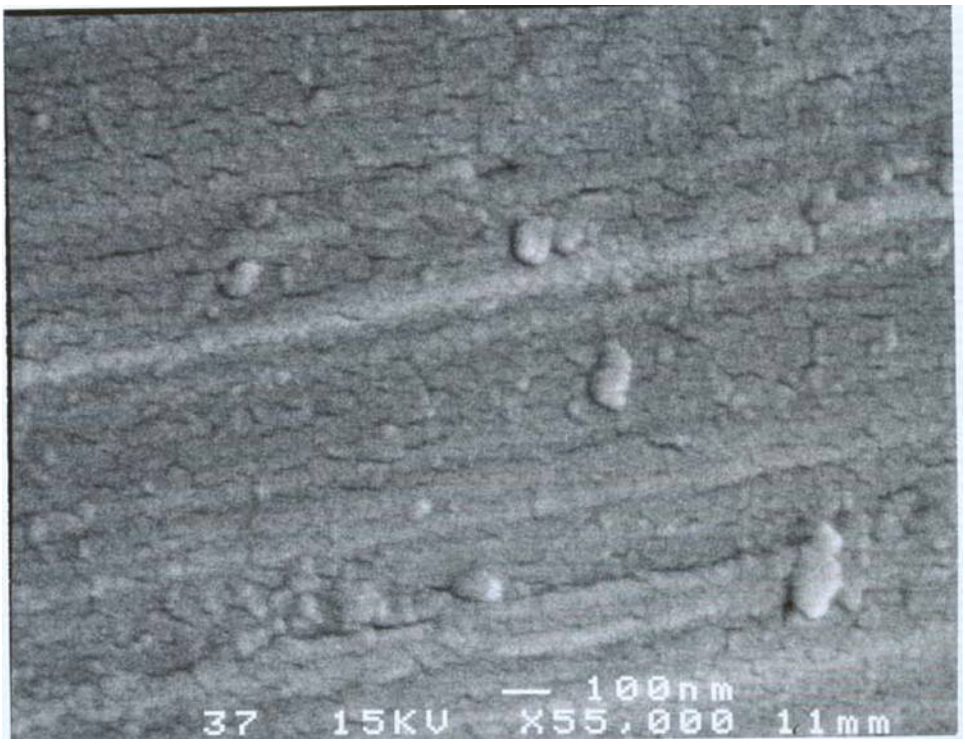

Fig. 7 SEM image of a raw aluminum foil, 55,000 X

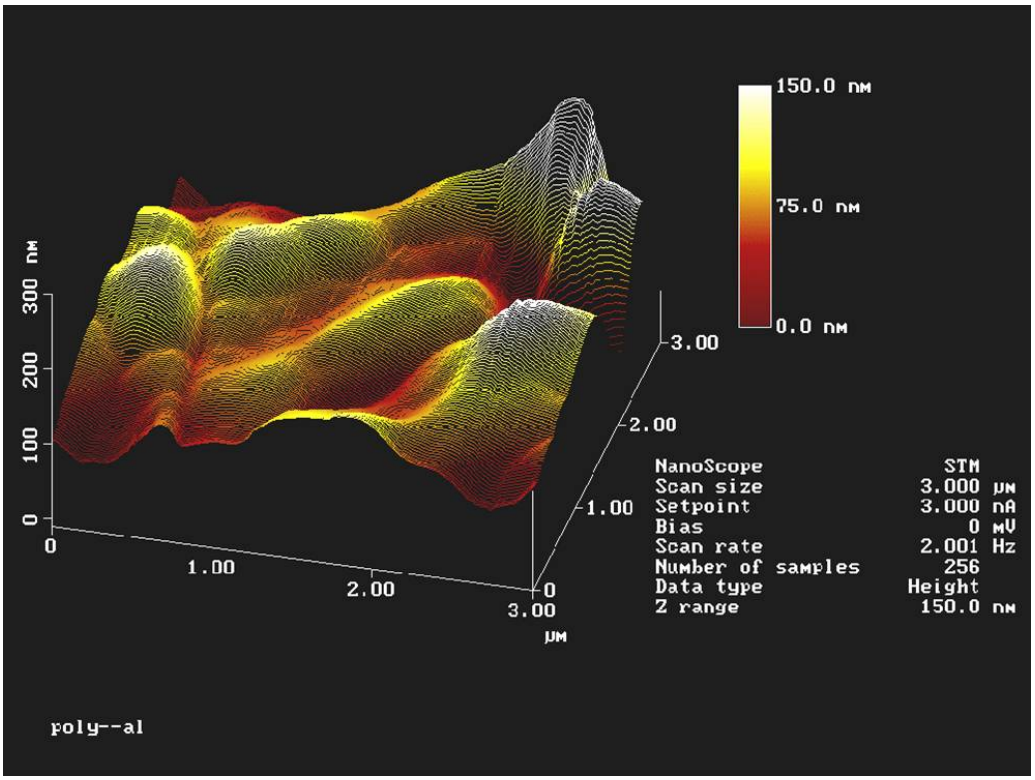

Fig. 8 AFM image of a raw Al foil, RMS roughness is 37.84 nm over 3x3 um, Zrange is 383.61 nm

Fig. 9 Electropolished, x25,000, 10 min, ~ 3.5V, room temperature

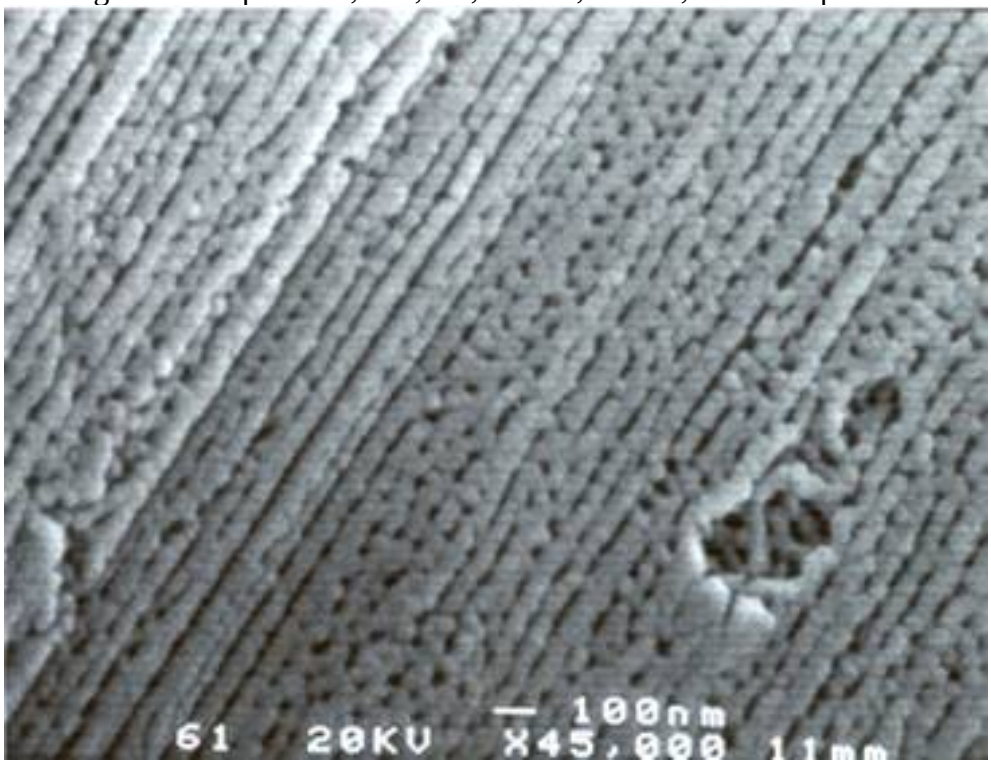

Fig. 10 SEM top view of a porous alumina template at 45,000X, degreased with acetone, anodized in oxalic acid for 2 hrs 38 mins at 27 °C, non-electropolished

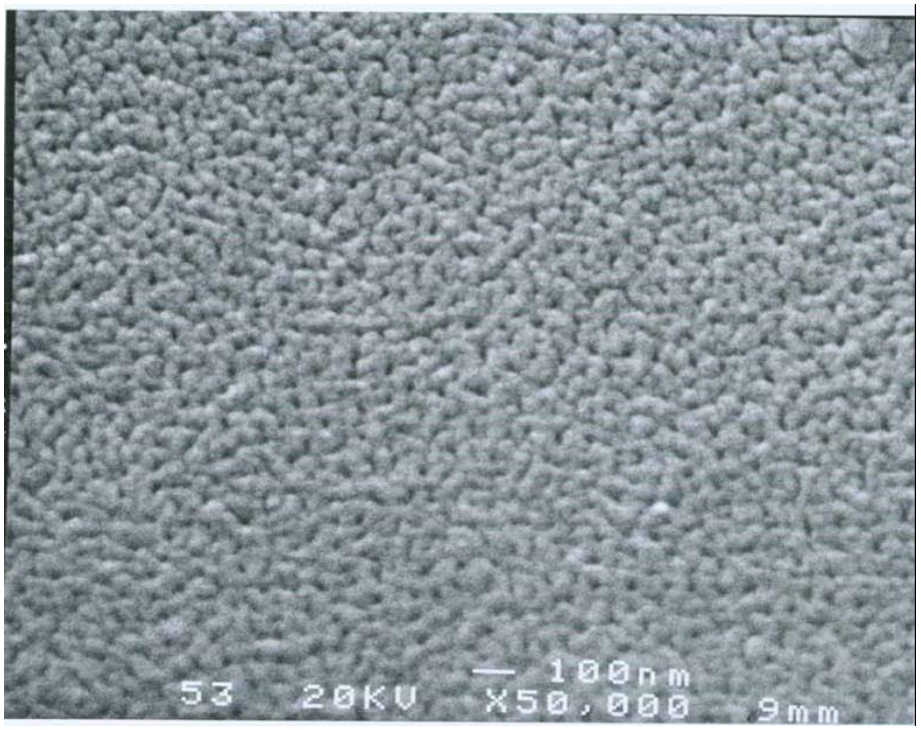

Fig. 11 Anodized, x 50,000, 0.3 M oxalic acid, 4 hrs, 40 V, ~7 °C

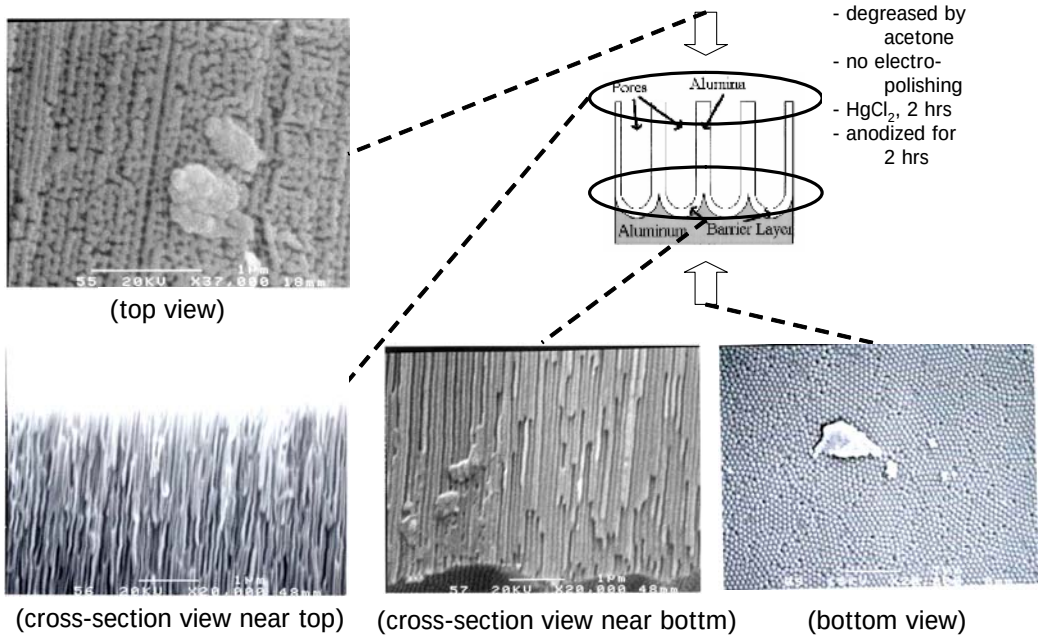

Fig. 12 Top, cross-section, and bottom view of the alumina template. The anodization was carried out according to process described in Section 2.1.

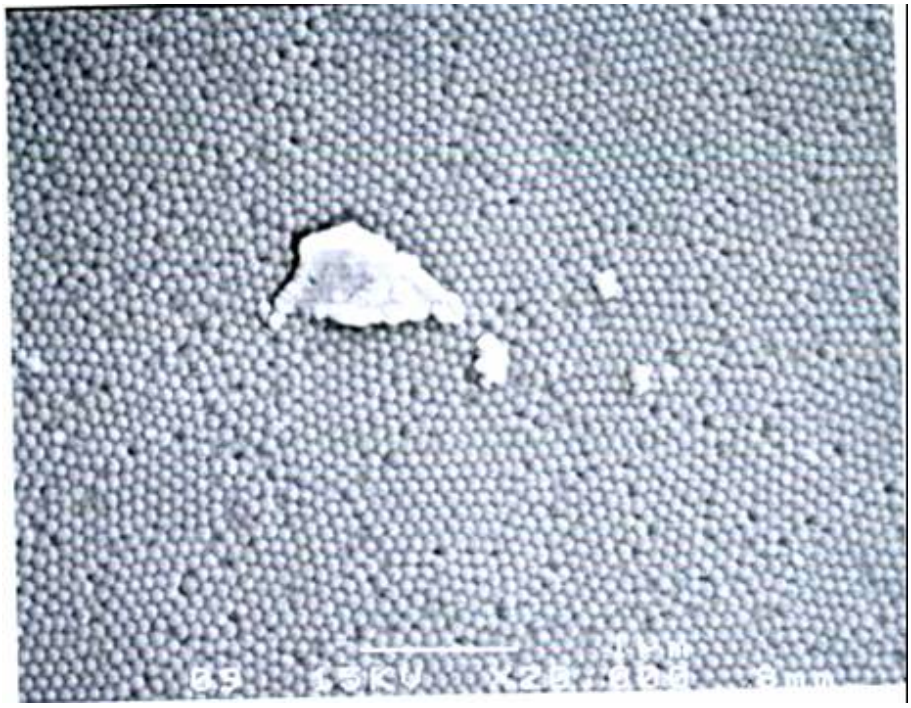

(a)

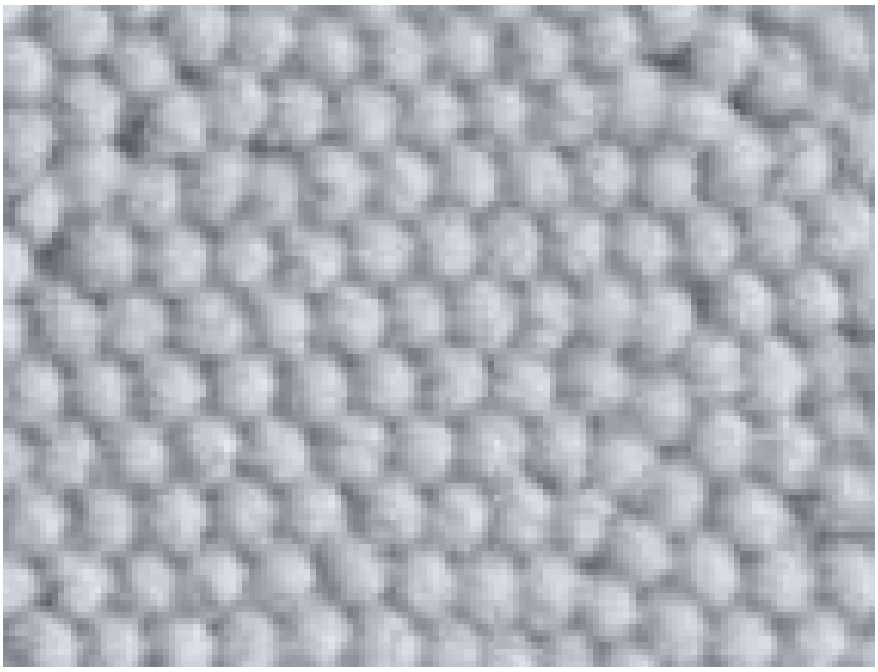

(b)

Fig. 13 (a) An SEM enlargement of bottom view of the template shows the polycrystalline arrangement of convex arrays before the removal of barrier layer. (b) A SEM enlargement of one domain of the template shows the almost perfect hexagonally ordered convex features. The cell size is about 100 nm.

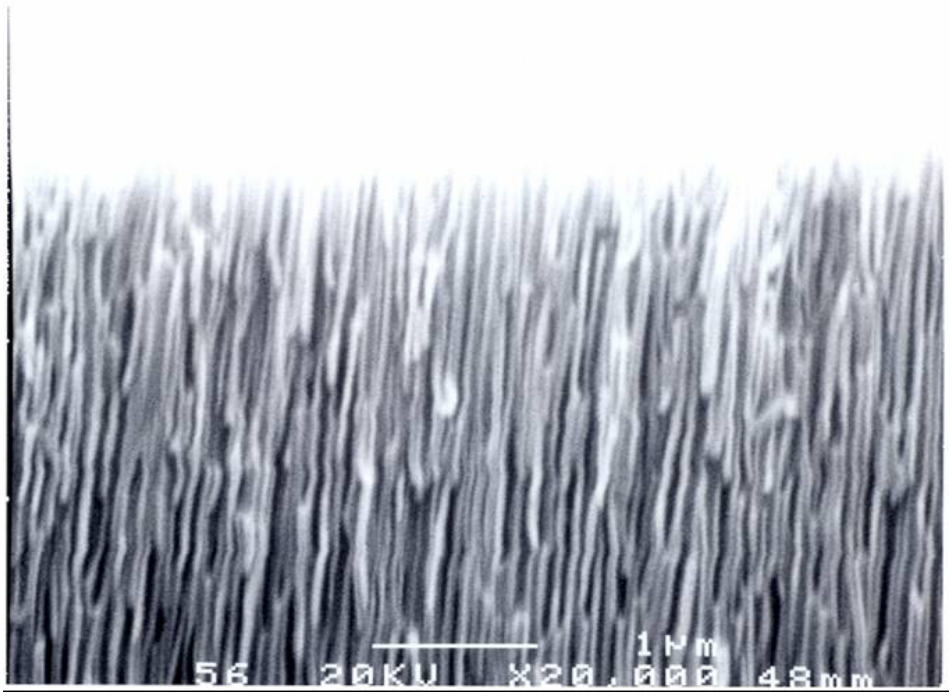

Fig. 14 An SEM enlargement of near-top cross section of the template shows the irregular pores, which were formed in the earlier stage of anodization.

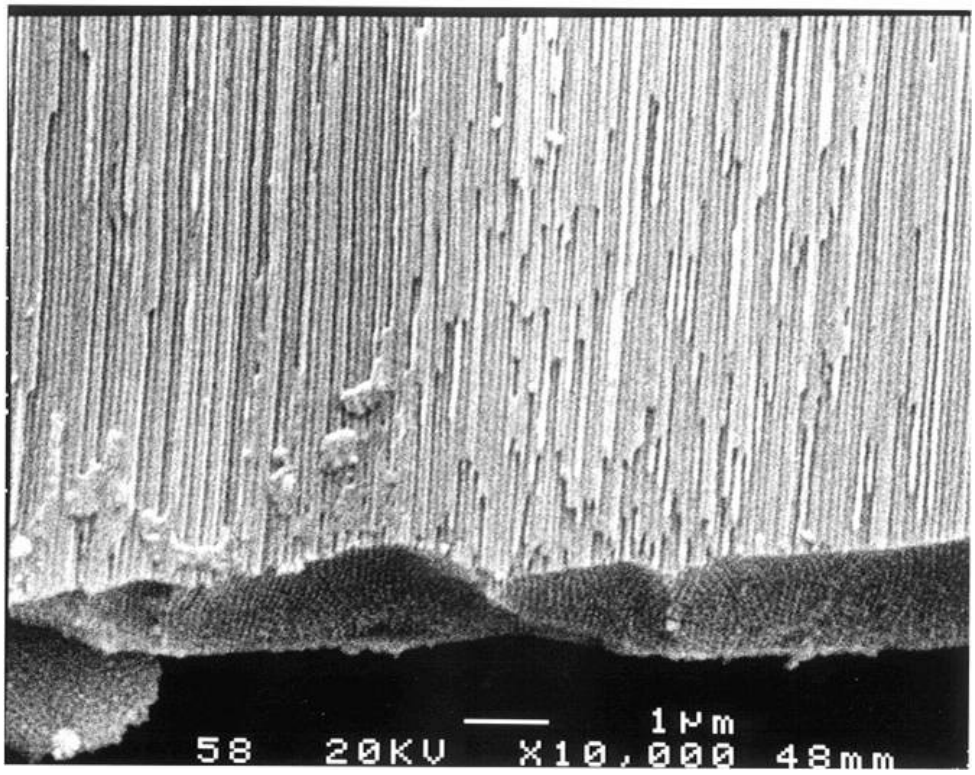

Fig. 15 An SEM enlargement of near-bottom cross section of the template shows the straight pores, which were formed in the later stage of anodization. The bottom surface is the barrier layer.

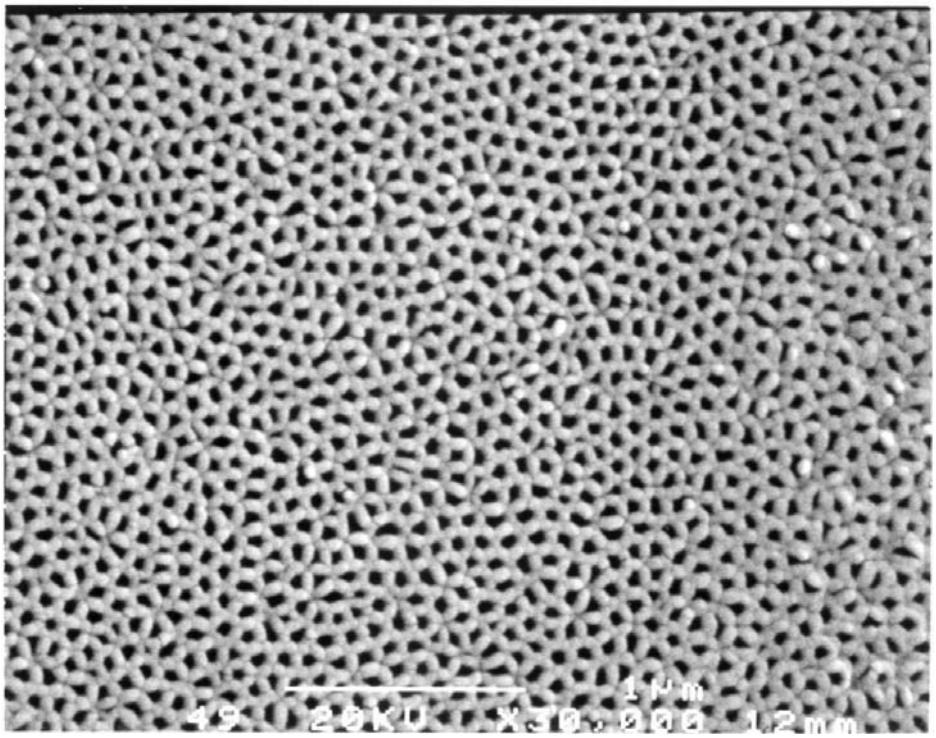

Fig. 16 An SEM of the bottom-view of the alumina template by single-step anodization. It was anodized in oxalic acid for about 23 hrs and was then dipped in a saturated $HgCl_2$ solution for about 1.5 hrs. The barrier layer was removed in 5% H_3PO_4 for 1.5 hours.

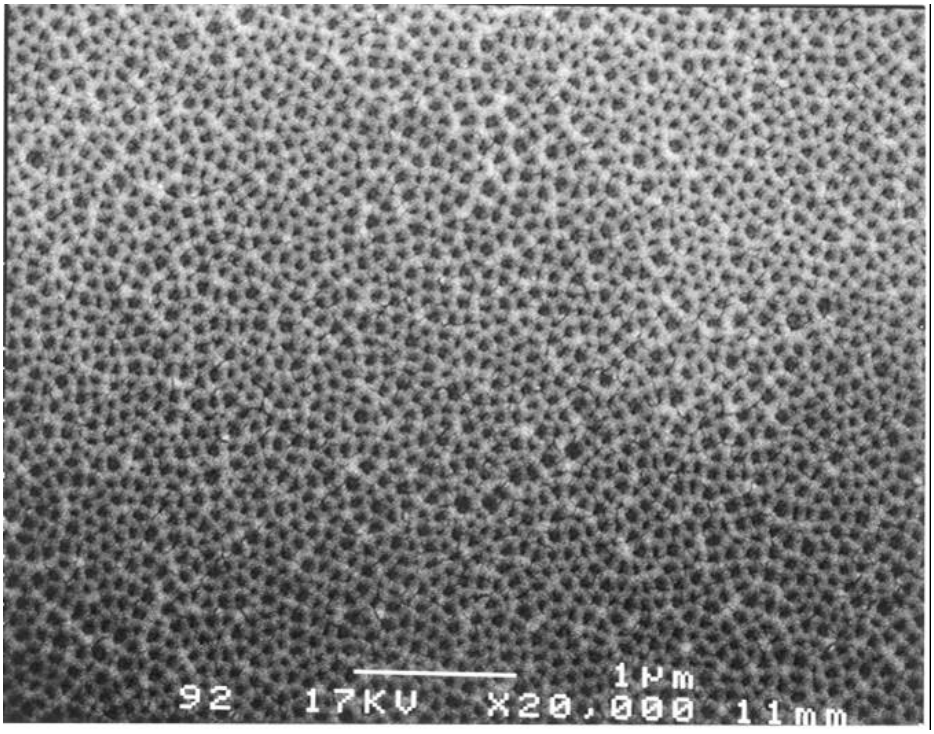

Fig. 17 An SEM of the "top-view" of the alumina template by two-step anodization. Note that the cell size and pore arrangement resemble those of "bottom-view" of the alumina template by single-step anodization.

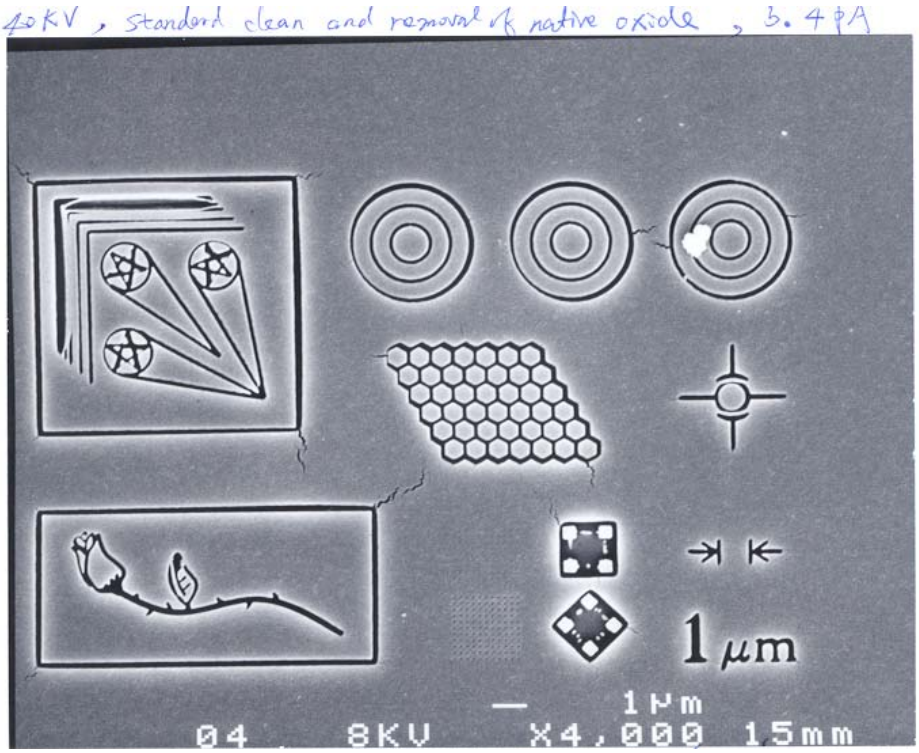

Fig. 18 Test pattern written on PMMA at 40 kV, beam current 5.4 pA, center-to-center exposure 7.08 nm, exposure time 412.1 usec, and dose: 2.91 nC/cm

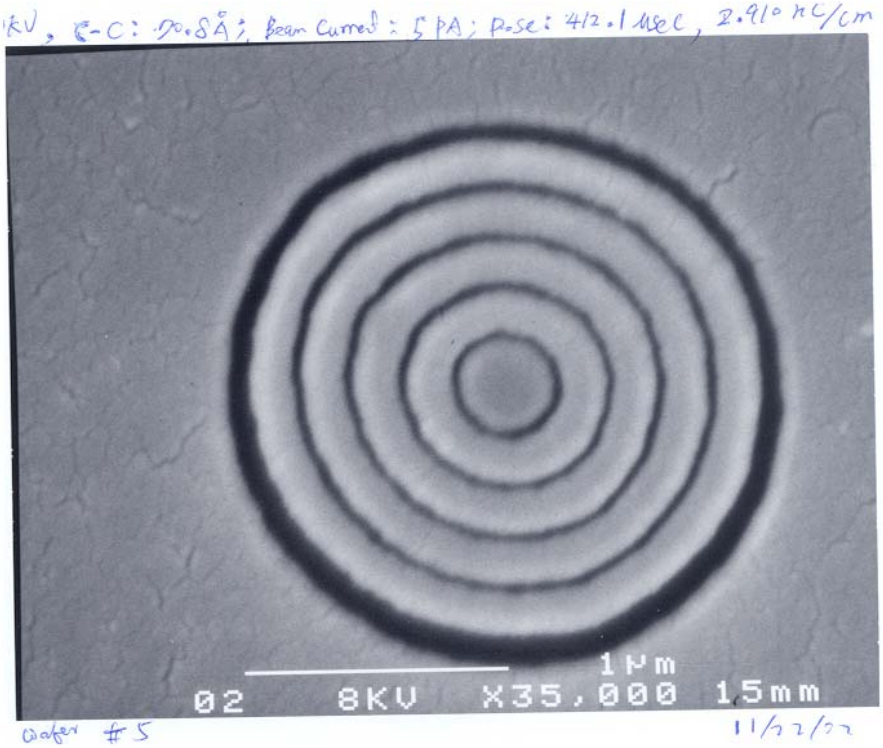

Fig. 19 Enlargement of the concentric circles in Fig. 18, showing the potential to write a pattern with as small as 30 nm lines.